

On the formation of compact, massive cores in stellar clusters and its relation with intermediate mass black holes

M. Arca-Sedda^{1,2*}

¹*Dept. of Physics, University of Rome Tor Vergata, Via Orazio Raimondo 18, I-00173, Rome (Italy)*

²*Dept. of Physics, University of Rome Sapienza, Piazzale Aldo Moro 5, I-00185, Rome (Italy)*

Revised to 02-2015

ABSTRACT

The recent discover of intermediate mass black holes (IMBHs) and dense compact objects in the centre of several galactic and extra-galactic stellar clusters opened a series of questions about their formation and evolution. One possibility is that gravitational encounters carry heavy stars to concentrate toward the cluster centre, leading to the formation of a compact sub-system composed mainly by high-mass stars. Correlations between those compact objects and the cluster in which they are contained could help to constraint their formation scenario. Using theoretical and statistical arguments, we show here that gravitational encounters lead to the formation of a dense system placed at the centre of the host stellar cluster. Moreover, we used one-to-one N -body realization of star clusters to follow the core formation process and its evolution. We derive scaling relations connecting the cluster mass and the deposited, central mass, comparing such results with observations. This work is the first showing that mass segregation in a stellar cluster gives rise, within the cluster centre, to a massive core whose mass correlates with the cluster mass as observations suggest.

Key words: stars: stellar evolution; stars: black holes; stars: kinematics and dynamics; galaxies: star clusters; Galaxy: globular cluster.

1 INTRODUCTION

Recently, it has been argued that some globular clusters (GCs) host a central black hole (BH). These BHs, with typical masses in the range $M \sim 10^2 - 10^4 M_\odot$, have been usually referred to as intermediate mass black holes (IMBHs), to distinguish them from stellar BHs ($M \sim 10 - 10^2 M_\odot$) and SMBHs contained within the nuclei of galaxies ($M \sim 10^6 - 10^{10} M_\odot$).

Many galactic and extra-galactic globular clusters seem to host IMBHs. As example, observations and modeling of the cluster M15 seems to be consistent with the presence of a compact central object (Gerssen et al. 2002; den Brok et al. 2014); the same result has been found for the cluster G1 in M31 (Gebhardt et al. 2002, 2005; Miller-Jones et al. 2012). Moreover, Noyola et al. (2008) found evidence for a BH with mass $\text{Log}(M/M_\odot) = 4.0_{-1.0}^{+0.75}$ in ω Centauri. Indications for an IMBH have been also found in other globular clusters in the Milky Way (Lützgendorf et al. 2013; Feldmeier et al. 2013).

On the other hand, many studies have shown that observational data can be interpreted as consequences of the presence of a small system composed by heavy objects

near the centre of the host cluster (Baumgardt et al. 2003; Kamann et al. 2014).

The interaction between an IMBH and the stars contained within the stellar system affects the dynamics within the cluster (Lützgendorf et al. 2013). Indeed, some works proposed that the evolution of stellar black hole binary (BHB), can constraint the upper limit of the mass of a central IMBH (Leigh et al. 2014).

The birth and growth of an IMBH can be attributed to merger events (Portegies Zwart et al. 1999; Goswami et al. 2012; Lützgendorf et al. 2015), or to a seed stellar BH that has grown through slow accretion (Miller & Hamilton 2002).

Another possibility is that gravitational encounters lead to an accumulation of mass within the cluster centre in form of orbitally decayed, massive stars.

In this framework, it is crucial to describe in detail the formation of stellar mass BHs, which is related both to the dynamical and stellar evolution of the stars moving within the cluster (Mapelli et al. 2013). On an observational side, moreover, it is very important to constraint the population of stellar BHs and the environment in which they evolve (Strader et al. 2012).

Gürkan et al. (2004) showed that rapid mass segregation can lead to the formation of a massive core within the cluster centre, whose mass correlates with the total mass of

* E-mail: m.arcasedda@gmail.com

the cluster. Such correlation is similar to that provided for black hole and the mass of the host clusters.

The dynamical evolution of a massive core formed in the centre of a stellar system, depends on the kind of initial mass function (IMF), which characterise the stellar content of the system itself.

As example, the core can harden through the physical process known as Spitzer instability (Spitzer 1940).

Considering two different mass population in a stellar environment, Spitzer (1940) showed that these populations tend to separate and evolve independently under some conditions, leading to the formation of a massive core composed by heavy stars which concentrates indefinitely and could lead to the formation of a seed IMBH.

The results found by Spitzer (1940) hold for a bimodal IMF, but recent works seem to indicate that a continuous IMF should enhance the instability (Trenti & van der Marel 2013; Arca-Sedda & Capuzzo-Dolcetta 2014b).

In this framework, we apply recent results concerning the dynamical friction process to show that it is possible to deposit a non negligible amount of mass in the centre of stellar clusters, in form of decayed stars, providing an explanation for the ever growing evidence of massive, compact objects in the centre of stellar clusters.

To give an estimate of the amount of stars which move toward the cluster centre, we resolve the cluster in all its stars, evaluating their dynamical decay time and comparing it with the stars life-time. Changing the mass and the initial mass function, the metallicity and the density distribution of each cluster allowed us to draw scaling relations between the cluster mass and the central mass, which we compared with observations for a wide set of different cluster models. Our results indicate that whenever the IMF of the stars is not a flat function, the deposited mass correlates with the cluster mass as the observed data suggest.

Moreover, we realised a reliable N -body modelling of two different star clusters, showing that mass segregation process leads to the formation of a very dense, contracting core composed by heavy stars.

The paper is organized as follows: in Section 2 is explained the methodology used to evaluate the deposited mass; in Section 3 is shown the sampling strategy followed to model the clusters and all the parameters used to characterise them; Section 4 is devoted to discuss the statistical results achieved while in Section 5 are shown results from direct N -body simulations; finally, in Section 6 will be drawn the conclusions.

2 DYNAMICAL FRICTION

The segregation of massive stars in the centre of stellar clusters is due mainly to the dynamical friction mechanism, which is a direct consequence of gravitational encounters with lighter stars (Chandrasekhar & von Neumann 1943; Chandrasekhar 1943a,b).

Dynamical friction mechanism acts on very different scales: from BH recoil in the centre of galaxies (Bekenstein 1973; Gualandris & Merritt 2008) to the decay of stellar cluster (Tremaine 1976; Capuzzo-Dolcetta 1993) and the formation of galactic nuclei (Milosavljević & Merritt 2001; Antonini 2013; Arca-Sedda & Capuzzo-Dolcetta 2014c).

Using the theory developed by Chandrasekhar (1943a), it is possible to obtain the timescale needed to a body of mass m_* , starting at position r_* with velocity v_* to decay toward the centre of its host system (Binney & Tremaine 2008):

$$t_{dyn}(\text{Myr}) = \frac{1.9 \times 10^4}{\log \Lambda} \left(\frac{r_*}{5 \text{ kpc}} \right)^2 \left(\frac{v_*}{200 \text{ km s}^{-1}} \right) \left(\frac{10^8 M_\odot}{m_*} \right), \quad (1)$$

where $\log \Lambda$ is the usual Coulomb logarithm and it is assumed, for star clusters, $\log \Lambda \sim 10$.

Many works have been devoted over time to generalise and improve the Chandrasekhar's work, in order to apply it to axisymmetric and triaxial systems (Binney 1977; Ostriker et al. 1989; Pesce et al. 1992), and to systems with cusped density profiles (Merritt et al. 2006; Vicari et al. 2007; Antonini & Merritt 2012; Arca-Sedda & Capuzzo-Dolcetta 2014a).

Arca-Sedda & Capuzzo-Dolcetta (2014a) developed a reliable treatment of df, providing a useful formula for the dynamical friction timescale:

$$t_{dyn}(\text{Myr}) = 0.3 \sqrt{\frac{R_g^3}{M_g}} (2-\gamma) g(e) \left(\frac{m_*}{M_{GC}} \right)^{-0.67} \left(\frac{r_*}{r_{GC}} \right)^{1.76}, \quad (2)$$

where m_* and r_* are the mass and the initial position of the traveling body, respectively, and $g(e) = (4.93 - 3.93e)$ is a linear function of the initial eccentricity of the orbit (e). Moreover, γ represents the slope of the density profile, while M_{GC} is the mass of the cluster and r_{GC} its scale radius. Finally, $R_g = r_{GC}/1$ kpc is the scale radius characterising the background in unit of kpc and $M_g = M_{GC}/10^{11} M_\odot$ is the cluster mass conveniently rescaled.

It is worth noting that the time needed to a massive star ($m_* \sim 25 M_\odot$) to decay in a GC ($M_{GC} \sim 10^6 M_\odot$), modeled with a $\gamma = 0$ profile, starting at $r = 5 \text{ pc}$ from the centre in circular orbit is:

$$t_{dyn} < 1 \text{ Gyr}, \quad (3)$$

using either Equation 1 and 2. This indicates that it is possible to obtain a population of stars concentrated into the centre of the cluster in few Gyr.

This convinced us to investigate whether or not the dynamical decay of massive stars within the cluster could lead to the formation of a compact stellar object, which could be the progenitor of an IMBH.

To do this, we sampled several cluster models of different masses resolving them in single stars, and then we estimate as a function of time, the fraction of stars with t_{dyn} smaller than the considered time. As it will be deepen in the following, in this process we considered also the stellar evolution mechanism, which changes the star masses and then changes the value of t_{dyn} and affects the estimation of the mass deposited within the cluster centre.

3 SAMPLING METHOD

As database to compare our results, we used the data provided in Lützgendorf et al. (2013) (hereafter LU13), which reported estimates of central mass excess, interpreted in that paper as BHs, for 14 GCs. Masses of the GCs and the BHs, or their upper limits, are shown in Table 1.

Table 1.

Parameters of the observed GCs collected in LU13.

ID	NAME	$\text{Log}(M_{GC}/M_{\odot})$	$\text{Log}(M_{BH}/M_{\odot})$
G1		6.76	4.25
NGC104	47Tuc	6.04	< 3.17
NGC1851		5.57	< 3.3
NGC1904	M79	5.15	3.47
NGC2808		5.91	< 4
NGC5139	ω Cen	6.40	4.6
NGC5286		5.45	3.17
NGC5694		5.41	< 3.9
NGC5824		5.65	< 3.78
NGC6093	M80	5.53	< 2.9
NGC6266	M62	5.97	3.3
NGC6388		6.04	4.23
NGC6715	M54	6.28	3.97
NGC7078	M15	5.79	< 3.64

Column 1: name of the cluster. Column 2: other name of the cluster. Column 3: mass of the cluster. Column 4: mass of the central BH.

To model the clusters, we used either a random spatial distribution and a cored Dehnen density profile ($\gamma = 0$) with masses, M_{GC} , in the range $10^3 - 3 \times 10^6 M_{\odot}$. For each cluster model, we sampled mass, position and eccentricity of each star belonging to it.

Eccentricities are sampled randomly, while positions are sampled according to the density profile of the system, which is, as stated above, a cored γ -profile or a flat distribution.

Masses of the stars are selected in three different ways in the range $0.1 - 100 M_{\odot}$: i) randomly, ii) following as initial IMF a Salpeter function (Salpeter 1955) and iii) following as initial IMF a Kroupa function (Kroupa 2001).

Moreover, we take in account the evolution of stars and mass loss taking advantage from the package SSE (Hurley et al. 2000), which we integrated in our code to provide the structural evolution of the star as function of time. Finally, in order to consider the effect of the metallicity, each cluster of each model mentioned above has been simulated with two different values of the metallicity, Z ; we selected $Z = 0.02$, which is really close to the value estimated in the solar neighborhood, and $Z = 0.0004$, which is the typical metallicity of old globular clusters.

At the end, we gathered a total sample of 12 models for any given mass of the cluster, whose main parameters are resumed in Table 2. Each model is labelled with letter A or B and a number from 1 to 6. Letter A indicates the models with solar metallicity, while letter B indicates metal-poor models. The number, instead, depends on the kind of IMF and the spatial distribution of the stars. We used three IMFs: random (denoted with letter R), Kroupa (K) and Salpeter (S). The spatial distribution considered, instead, is random (R) or Dehnen-like (D).

4 RESULTS

To give an estimate of the mass of the cluster core, it is needed a detailed description of the stellar evolution process, which cause the star mass loss and can affect both the dynamical friction efficiency and the amount of mass carried

Table 2.

Parameters of the cluster models.

Model	IMF	$\rho(r)$	Z	$M_{GC} (M_{\odot})$
A1	K	R	0.02	$10^3 - 3 \times 10^6$
A2	K	D	0.02	$10^3 - 3 \times 10^6$
A3	S	R	0.02	$10^3 - 3 \times 10^6$
A4	S	D	0.02	$10^3 - 3 \times 10^6$
A5	R	R	0.02	$10^3 - 3 \times 10^6$
A6	R	D	0.02	$10^3 - 3 \times 10^6$
B1	K	R	0.0004	$10^3 - 3 \times 10^6$
B2	K	D	0.0004	$10^3 - 3 \times 10^6$
B3	S	R	0.0004	$10^3 - 3 \times 10^6$
B4	S	D	0.0004	$10^3 - 3 \times 10^6$
B5	R	R	0.0004	$10^3 - 3 \times 10^6$
B6	R	D	0.0004	$10^3 - 3 \times 10^6$

Column 1: name of the model. Column 2: IMF used to sample masses of the stars. Column 3: spatial density profile of the stars. Column 4: metallicity of the cluster. Column 5: masses of the cluster models.

to the centre of the cluster. To account for stellar evolution we used the package SSE, which allowed us to get stellar parameters along the whole simulated time for each star and each cluster.

In the following, to reduce the number of graphs, we use as reference cases the models A1 and B1 (see Table 2) considering a cluster with $M_{GC} = 5 \times 10^3 M_{\odot}$.

Since we found that the deposited mass saturates to a nearly constant value after ~ 3 Gyr from the start of the evolution, in the following we will refer to our results considering as minimum age of the cluster $t = 5$ Gyr, in order to obtain results compatible either with very old clusters (with ages ~ 10 Gyr) and younger star clusters.

Figure 1 shows the initial versus final mass of the stars within the cluster.

Stars with decay times smaller than 5 Gyr have masses above $20 M_{\odot}$ unless a small population of low mass stars which are located initially very close to the cluster centre.

Moreover, stellar observables can be useful to determine which kind of stars we find in the inner region of the cluster. In Figure 2 are shown the H-R diagrams of the cluster in A1 and B1 models at time $t = 5$ Gyr, in which are evident the main sequence (MS), the red giant branch (RGB), the asymptotic giant branch (AGB), a large white dwarves sequence and few, very faint, objects.

Looking at Figure 3, which shows the kind of stars within the cluster used as reference, it is easier to understand which kind of stars we expect to find in the core of the cluster. The population of decayed stars is dominated by neutron stars and black holes, but also low mass main sequence stars seem to play a minor role. The reference names for each evolutionary phase is the same as in Hurley et al. (2000) and they are resumed in Table 3.

The contribution given by stellar BHs is more evident in Figure 4, in which is shown the number of BHs as function of the cluster mass. It is clear a certain correlation between the two quantities; moreover, passing from higher to smaller Z (from model A1 to B1), the number of produced BHs slightly increase.

Despite the useful informations provided by the SSE

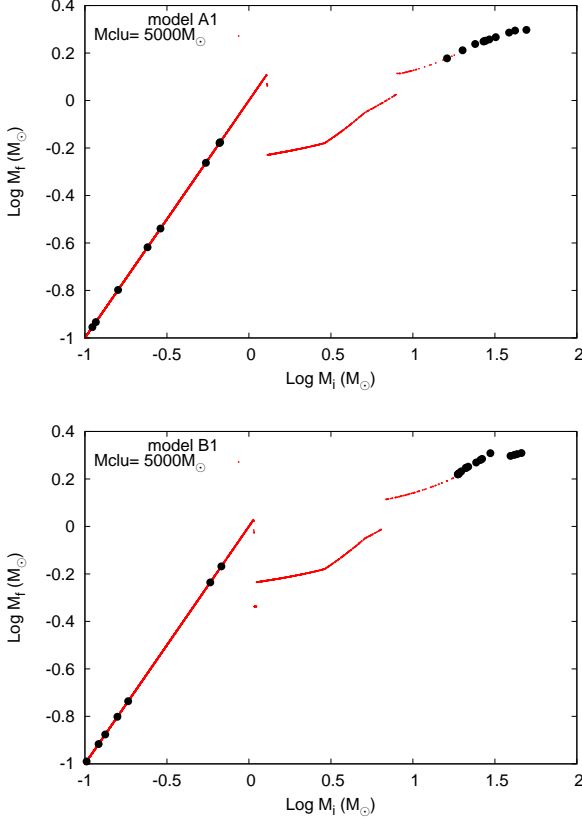


Figure 1. Final versus initial mass of stars in a cluster of $5 \times 10^3 M_\odot$. In this case, we selected as IMF the Kroupa function. Black dots label the decayed stars.

package, the main aim of this work is to draw scaling relations between the core formed by decayed stars and the mass of the cluster to compare with the data in LU13. Figures 5 and 6 show such correlations for all the models considered.

Moreover, Table 5 reports the parameters obtained by fitting our correlations with a relation:

$$\text{Log}(M_{cen}/M_\odot) = a\text{Log}(M_{GC}/M_\odot) + b, \quad (4)$$

with M_{cen} the deposited mass and M_{GC} the mass of the cluster. Parameters obtained by LU13 using the same fitting relations are reported in Table 6.

Concerning the models with solar metallicity (models A1-A6), we see that the best agreement between the observations and our estimate are obtained for models A1 and A2, which are models characterised by the Kroupa IMF and in which the stars are distributed in the space randomly (model A1) or according to the Dehnen density profile (model A2). The models A3-A4 still seem to be comparable with observations, despite the predicted central mass is slightly higher than observed data. On the other hand, models A5-A6, in which masses for the stars are sampled randomly, cannot explain the mass observed in the dataset of LU13. This result is an additional proof that the masses of stars in clusters should follow a non-flat IMF.

Concerning instead the models with low metallicity (B1-B6), we notice that the results do not change significantly with respect results found in A-models. In particular,

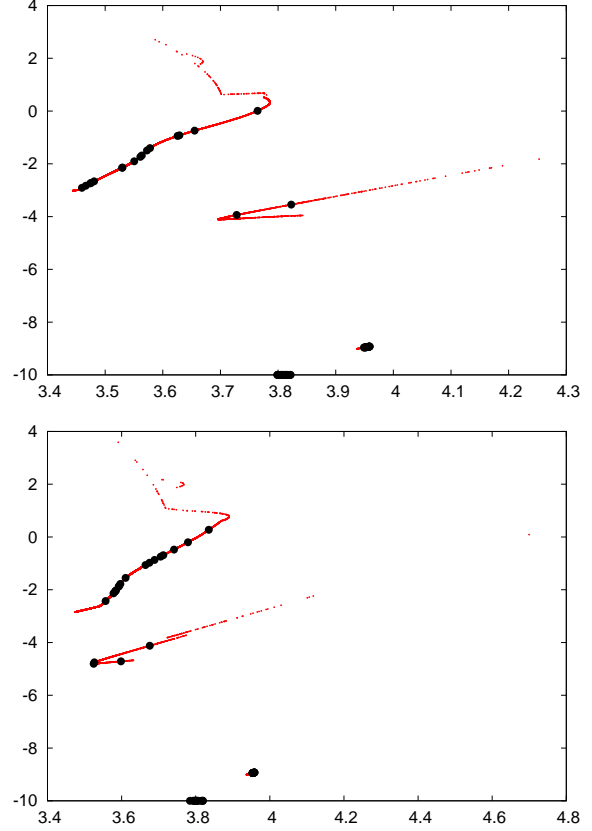


Figure 2. H-R diagram of the cluster with mass $M_{GC} = 5 \times 10^3 M_\odot$. In this case, we selected as IMF the Kroupa function. Black dots label the decayed stars. In the top panel, we assumed $Z = 0.02$ while in the bottom panel $Z = 0.0004$.

Table 3.

Evolution phase of the stars (see also Hurley et al. (2000)).

REF N.	NAME	Description
0	MSI	MS stars with $M \leq 0.7 M_\odot$
1	MSh	MS stars with $M > 0.7 M_\odot$
2	HG	Hertsprung Gap
3	GB	First GB
4	CHeB	Core Helium Burning
5	EAGB	Early AGB
6	TPAGB	Thermally Pulsing AGB
7	HeMS	Naked Helium star MS
8	HeHG	Naked Helium star Hertsprung Gap
9	HeGB	Naked Helium star GB
10	HeWD	Helium White Dwarf
11	COWD	Carbon/Oxygen White Dwarf
12	ONeWD	Oxygen/Neon White Dwarf
13	NS	Neutron Star
14	BH	Black Hole
15	m0	massless remnant

Column 1: reference number used in Hurley et al. (2000). Column 2: abbreviation. Column 3: evolution phase.

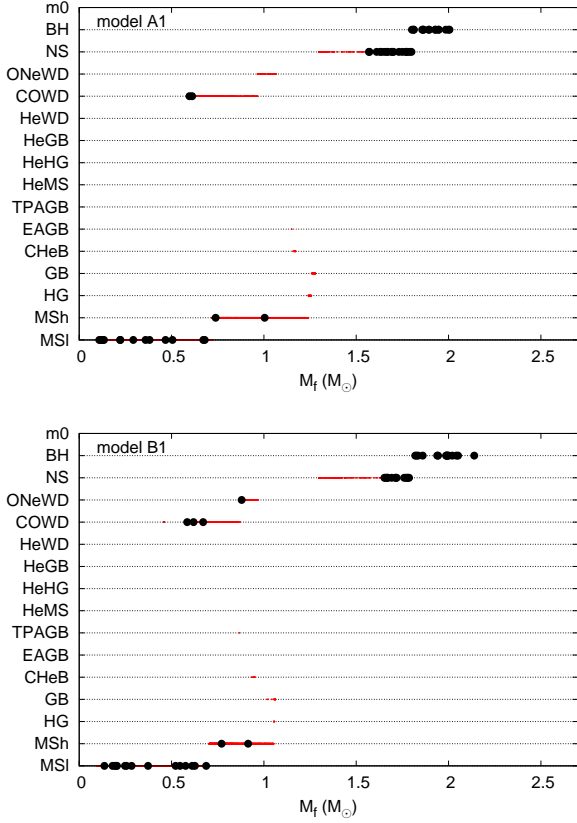


Figure 3. Kind of the decayed stars (labeled with an integer from 0 to 14) with respect to the final mass of the stars in a cluster with $M_{GC} = 5 \times 10^3 M_\odot$. In the top panel, we assumed $Z = 0.02$ while in the bottom panel $Z = 0.0004$.

the low metallicity models produce cores typically greater than the solar metallicity ones, with a difference of $\sim 15\%$.

This can be explained looking at Figure 7, which shows the initial and final mass of stars sampled with the Kroupa IMF considering different values of Z . Looking at this graph, it is evident that the final mass of decayed stars with low Z are 15% smaller than the values obtained for stars with solar Z . Since it has been shown that the metallicity could be important in determine the final mass of the star, especially for massive stars with low metallicity (Brocato et al. 1999; Mapelli & Bressan 2013; Ziosi et al. 2014), it would be worth to investigate how the usage of different stellar evolution recipes could affect our results.

Although the results carried out in this section provide useful hints about the formation of massive cores in star cluster on a wide range of masses and in many different cases, it cannot provide informations about the structure of those cores, neither on the possible formation of an IMBH in the cluster centre. Due to this, we performed two direct N -body simulations of two reliable star cluster models, in order to support our statistical results and to follow the formation process of the core and its evolution. Next section is devoted to present and discuss the results obtained from the direct simulations.

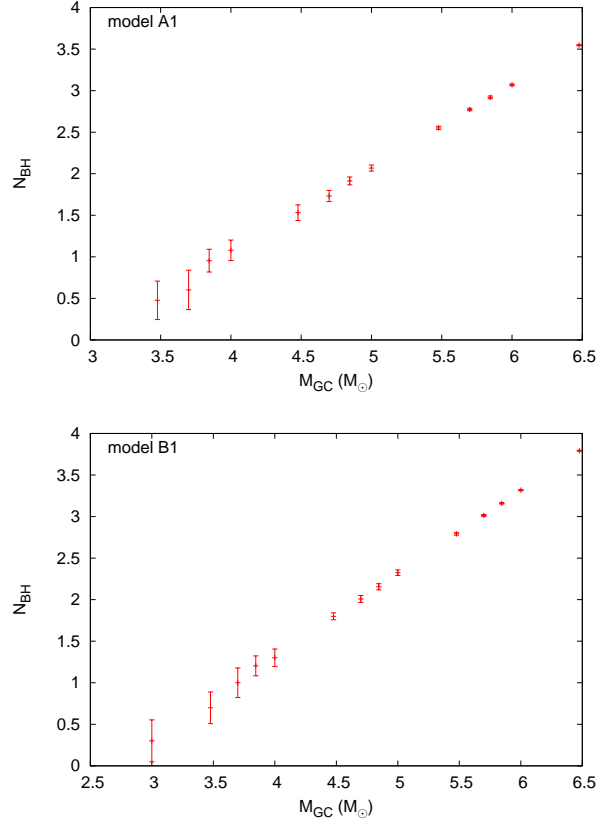


Figure 4. Number of black holes produced as function of the mass of the cluster. In this case, we selected as IMF the Kroupa function. In the top panel, we assumed $Z = 0.02$ while in the bottom panel $Z = 0.0004$.

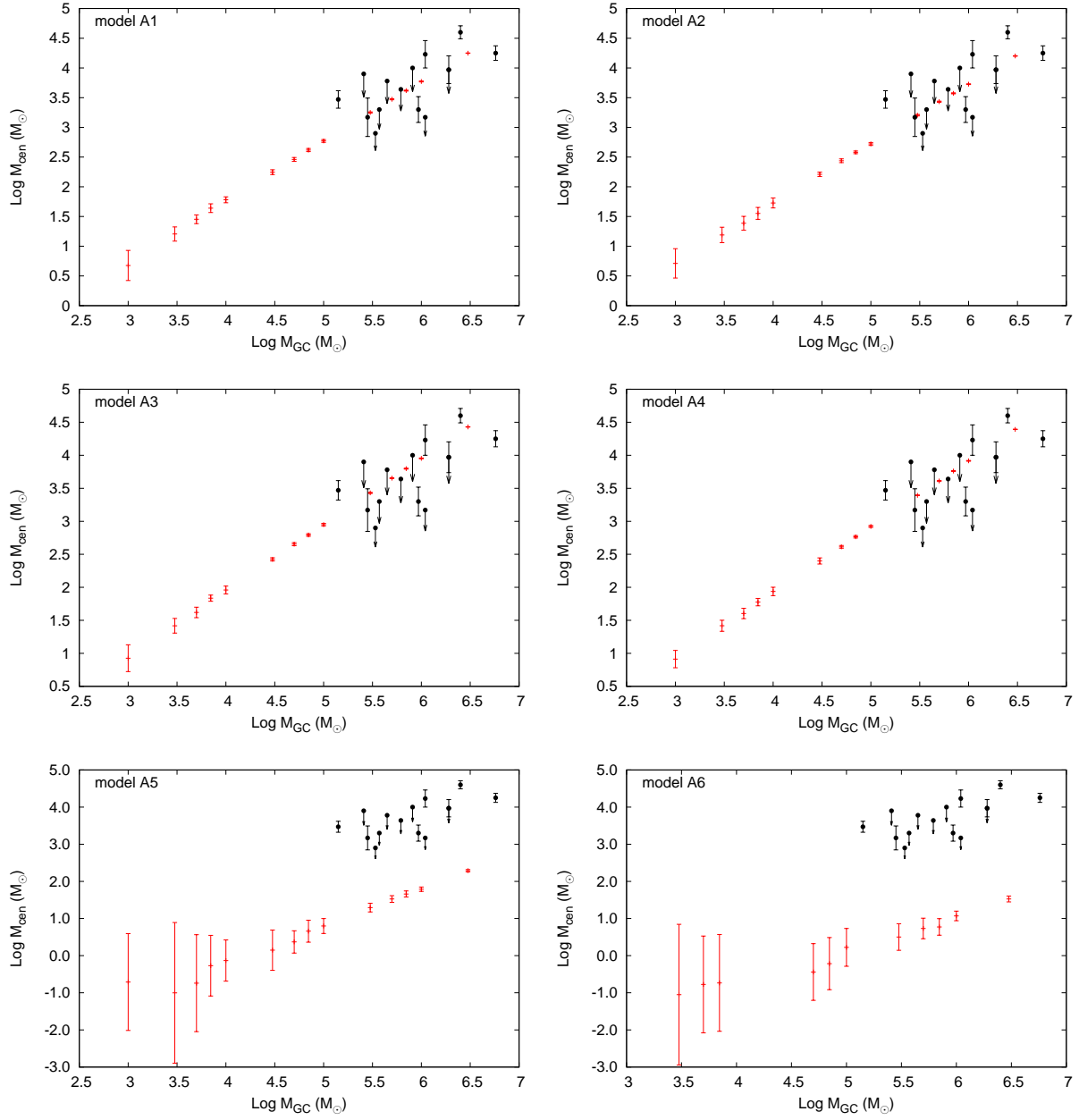


Figure 5. Segregated mass vs the total mass of the cluster. Black dots represent observative data. All the models here have solar metallicities.

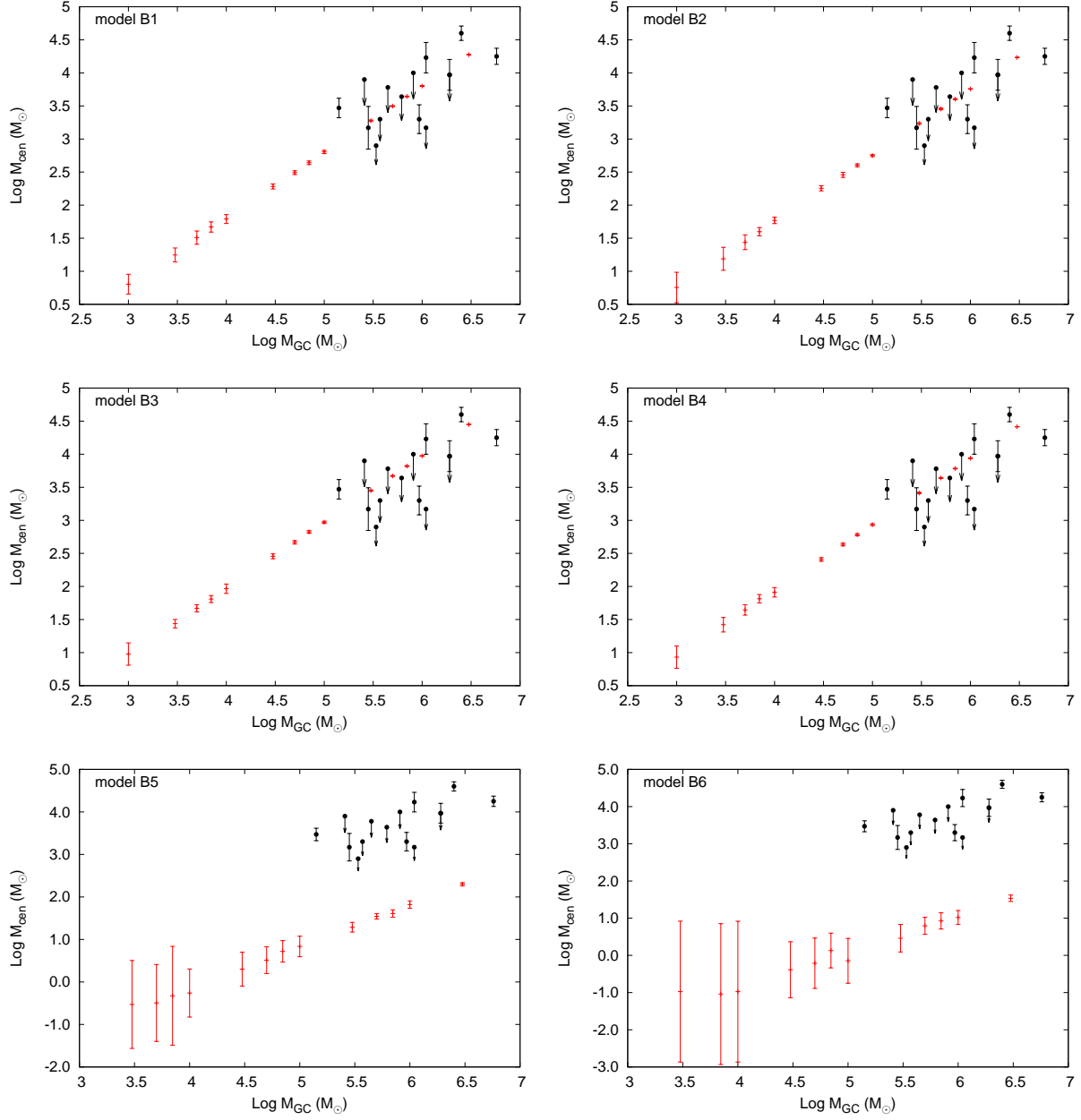


Figure 6. Segregated mass vs the total mass of the cluster. Black dots represent observative data. All the models here have metallicities $Z = 0.0004$.

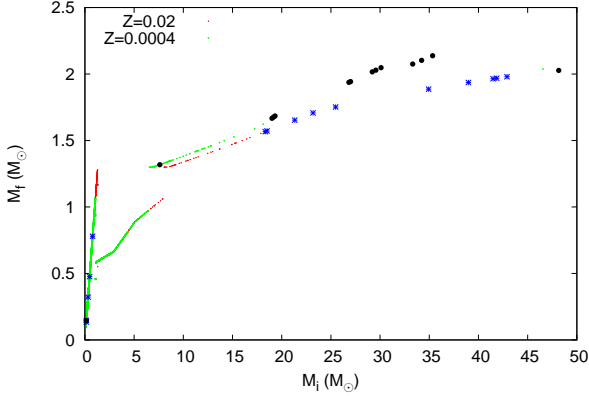


Figure 7. Initial and final mass of the all and decayed stars in a cluster model with $M = 10^5 M_\odot$ and with $Z = 0.02$ (red and blue dots, respectively) and $Z = 0.0004$ (green and black dots, respectively).

5 N-BODY MODELLING OF A STELLAR CLUSTER: IMF, MASS SEGREGATION AND CORE FORMATION

In this section we provide preliminary results of direct N -body simulations, which deserve to support the statistical results presented above. In fact, these simulations allow to follow the dynamical evolution of star clusters and may provide useful informations about the possible formation of compact structure within the cluster centre.

In particular, we ran two different simulations, to which we refer hereafter as NB1 and NB2. To model the cluster we used the density profile:

$$\rho(r) = \rho_0 \left(\frac{r}{r_{GC}} \right)^{-\gamma} \left(\frac{r}{r_{GC}} + 1 \right)^{-4+\gamma} \cosh^{-1}(r/r_{cut}), \quad (5)$$

where $\rho_0 = [(3 - \gamma)M_\infty]/[4\pi r_{GC}^3]$ is the scale density, M_∞ the total mass of the model, r_{GC} its scale radius, and r_{cut} the truncation radius. If $r_{cut} \gg r_{GC}$, this density profile is equal to the so-called Dehnen density profile (Dehnen 1993).

In this case, we used $r_{cut} = 10 pc$, in order to obtain a model whose radial extension is compatible with real star clusters. The total mass of the system obtained this way is labelled with M_{GC} , in agreement with the convention used in the other sections.

In simulation NB1, the cluster has been modeled with $N = 262, 144$ particles whose masses were sampled through the Salpeter IMF. Sampling the particle masses in the range $[0.1 - 100] M_\odot$, we obtained a cluster with total mass $M_{GC} = 90, 130 M_\odot$.

The cluster in simulation NB2, instead, has been modeled with $N = 524, 288$ particles and using as initial IMF a Kroupa function. Even in this case, the mass of each particle has been sampled in the range $[0.1 - 100] M_\odot$, leading to a cluster of mass $M_{GC} = 334, 725 M_\odot$.

Table 4 resumes the main parameters which characterise the NB1 and NB2 simulations.

The simulations have been performed by means of HiG-PU's (Capuzzo-Dolcetta et al. 2013), a direct, high-precision, N -body integrator which fully exploits the advantages of parallel computing. We used as gravitational softening $\epsilon =$

Table 4.

Parameters of the N -body simulations.

Model	IMF	γ	r_{GC} (pc)	M_∞ (M_\odot)	M_{GC} (M_\odot)	N
NB1	S	0	0.7	102, 180	90, 130	262, 144
NB2	K	0	1.6	500, 000	334, 725	524, 288

Column 1: . Column 2: IMF used to sample the mass of each star: Salpeter (S) or Kroupa (K) function. Column 3: slope of the model density profile. Column 4: scale radius of the model in pc. Column 5: mass of the cluster for $r_{cut} \rightarrow \infty$. Column 6: mass of the cluster actually sampled. Column 7: number of particles used.

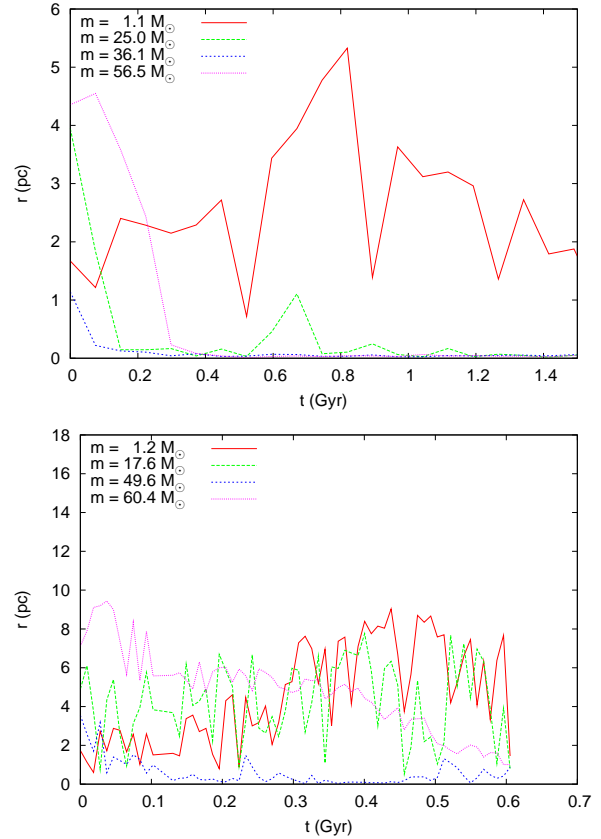


Figure 8. Radial distance, as function of time, of some stars in simulation NB1 (top panel), and NB2 (bottom panel).

0.05 pc both in simulations NB1 and NB2, allowing a reliable description of the motion of stars on this length scale.

Figure 8 shows the distance from the centre of the cluster, as function of time, of stars with different masses in NB1 and NB2 configurations. It is quite evident that stars with masses above $20 M_\odot$ suffer a strong dynamical friction, which lead the heavy stars toward the cluster centre in less than 1 Gyr, in agreement with Equation 1. On the other hand, dynamical friction does not affect the motion of low-mass stars, which moves on random trajectories dominated by gravitational encounters.

On a global scale, the deposit of mass within the cluster centre can be shown through the evolution, as function of time, of the half-mass radius, r_{50} . In particular, Figure 9

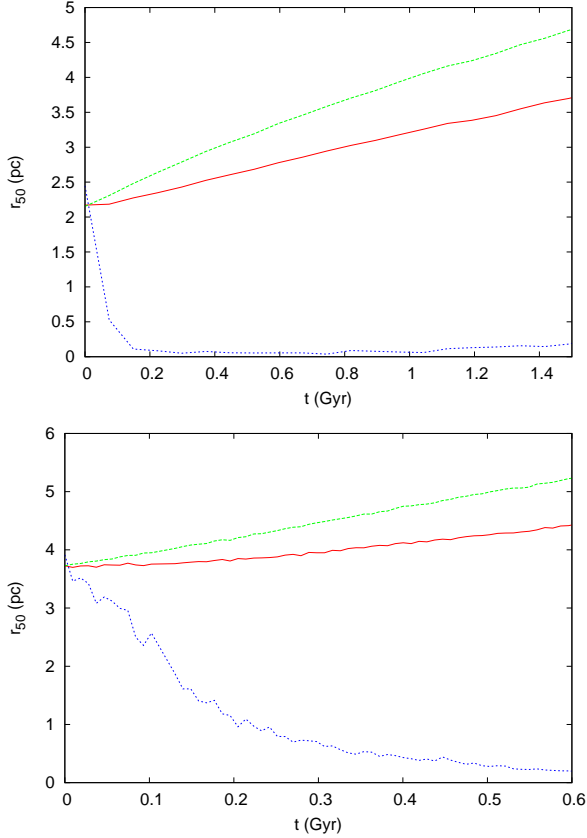


Figure 9. Radial distance, as function of time, of some stars in simulation NB1 (top panel), and NB2 (bottom panel).

shows r_{50} as function of time for the whole star cluster, the sub-system composed by stars lighter than $1 M_{\odot}$ and that composed by stars heavier than $30 M_{\odot}$, respectively. It is quite evident that heavy stars concentrate toward the center of the cluster on a time-scale $\lesssim 0.5$ Gyr both in NB1 and NB2 cases.

Concerning configuration NB1, the population of stars heavier than $30 M_{\odot}$ is composed by 68 stars and has a total mass of $3,162.7 M_{\odot}$. Such mass is confined, after ~ 2.5 Gyr, in a region with radial extension ~ 0.14 pc, while $r_{50} \sim 0.06$ pc, comparable to the gravitational softening used.

In configuration NB2, instead, the population of heavy stars (561 stars) has a total mass of $27,327 M_{\odot}$ and $r_{50} \sim 0.2$ pc, greater than in NB1 configuration, but in this case the model has been evolved only for 0.6 Gyr.

However, in both cases is evident a strong mass segregation, which leads the whole population of heavy stars to form a dense sub-system with a relatively small radial extension.

This is also made clear from Figures 10 and 11, which show the distribution of heavy stars on the x-y plane at the beginning and the end of the simulations.

The formation of a dense and massive sub-structure within the cluster can be also argued by looking at the radial, cumulative mass profile of the system, showed in Figure 12. Looking at this figure makes evident the formation of a mass excess in the centre of the cluster of $\sim 5 \times 10^4 M_{\odot}$ within 1 pc both in case NB1 and NB2.

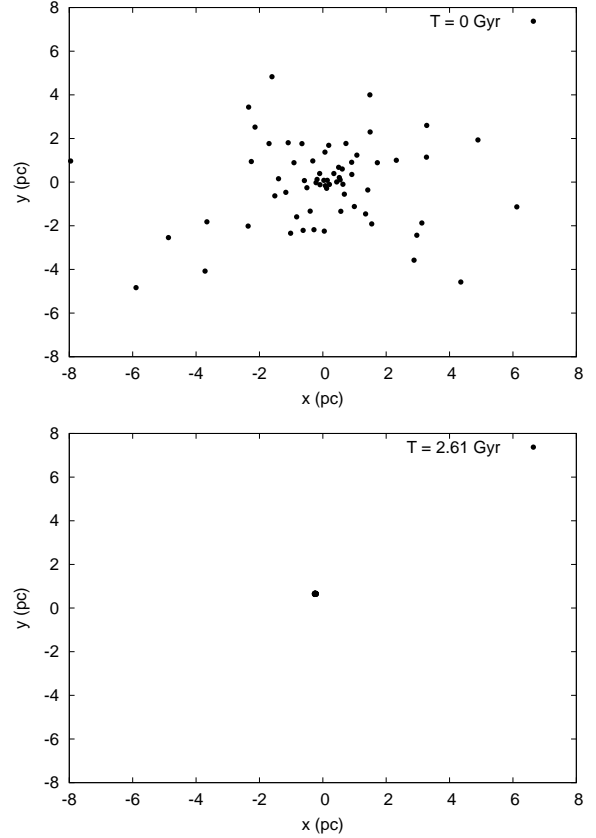


Figure 10. Distribution of stars with masses above $30 M_{\odot}$ in the x-y plane for configuration NB1 at $t = 0$ (top panel) and $t = 2.6$ Gyr (bottom panel). It is worth noting that at $t = 2.6$ Gyr the stars are all enclosed within a region whose radius is 0.14 pc.

The presence of a compact massive objects within the cluster centre may alter the dynamics of stars in this region, giving rise to an edge in the velocity dispersion profile of the cluster. For this reason, the presence of a central IMBH in star cluster is often inferred by the velocity dispersion profile (see as example Emsellem et al. (1994)), which allows to constrain its mass by solving the Jeans equations (Jeans 1916; Cappellari 2002).

However, as pointed out also in other works (see as example Baumgardt et al. (2003)) the edge in velocity dispersion profile can be attribute to a compact, dense system placed near the cluster centre. Figure 13 shows the 3D velocity dispersion of the clusters for cases NB1 and NB2. It is quite clear the formation of an edge within 1 pc from the cluster centre, essentially due to the formation of the compact sub-system of heavy stars.

Despite the formation of a massive core within the cluster centre may explain many observed velocity dispersion profiles, it does not exclude the possible subsequent formation of an IMBH through gravitational collisions and core hardening. Figure 14 shows the total energy of the system composed by heavy stars as function of time in configuration NB1 and NB2. The continuous decreasing corresponds to a continuous contraction of the core, and may lead to an enhancement of gravitational collision efficiency and, even, to the formation of a seed BH. However, such simulations are limited by the gravitational softening, ϵ , because of the fact

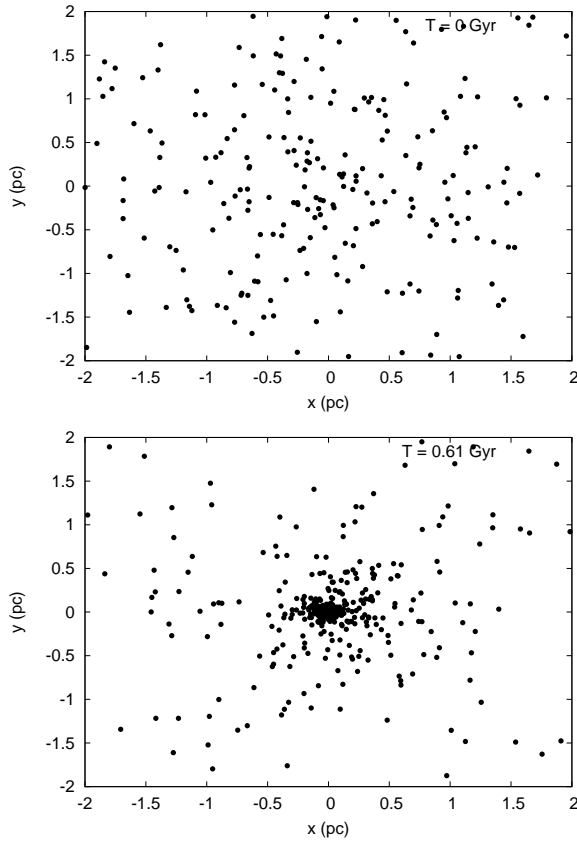


Figure 11. Distribution of stars with masses above $30 M_{\odot}$ in the x-y plane for configuration NB2 at $t = 0$ (top panel) and $t = 0.6$ Gyr (bottom panel). In this case stars are less concentrated than in case NB1, but the model has been evolved for a smaller time.

that the integrator does not ensure a reliable description of the dynamics as the core reaches dimension comparable to ϵ .

Therefore, at present we can only highlight that the heavy component of the system tends to separate from the cluster and evolves independently, leading to a massive core which contracts indefinitely, unless its dimension are comparable to the gravitational softening used. In a forthcoming paper, we will deepen the evolution of such cores, using appropriate numerical techniques to follow the dynamics also on very small scales, allowing us to put stronger constraint on the possible formation of IMBHs.

6 CONCLUSIONS

In this work we gave estimate of the mass which can be deposited in the centre of a stellar cluster as consequence of two-body interactions. Our results have been compared with observational data which indicate the presence of an IMBH in the centre of a sample of globular clusters. The comparison turned out that the mass excess could be attributed to the segregation of stars toward the cluster centre which leads to the formation of a massive core.

The correlations found between the mass of such core and that of the cluster are in good agreement with observations, unless the stars are distributed randomly within the

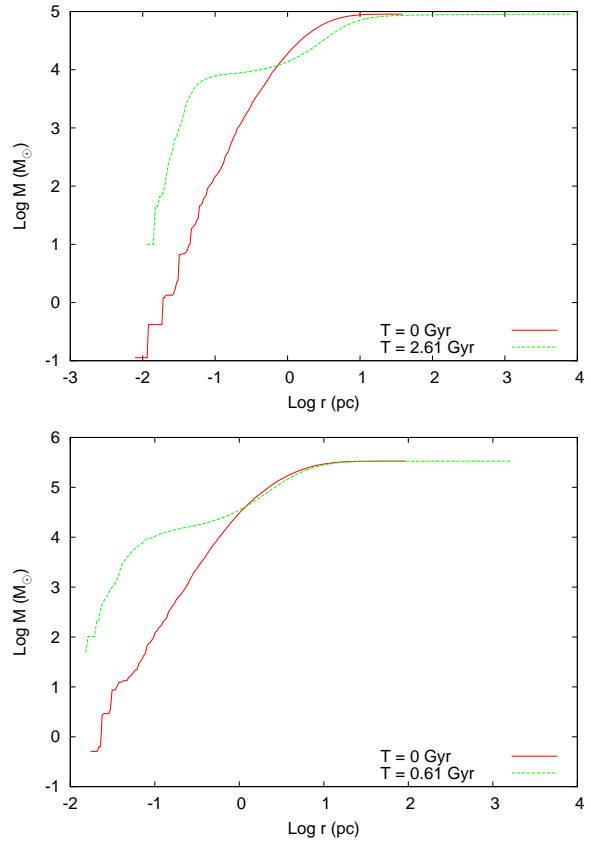


Figure 12. Cumulative mass profile of the star cluster in case NB1 (top panel) and NB2 (bottom panel).

cluster radius. In fact, the best agreement has been reached sampling the stars in the model with a Dehnen density profile for the spatial distribution and with the Kroupa IMF for the mass distribution.

We notice that results do not change significantly assuming for the cluster different metallicities.

We ran also direct N -body simulations which allowed us to follow the formation process of the core. Thanks to the high resolution provided by the optimized usage of hardware and software facilities, we were able to simulate the evolution of a reliable cluster model, using for the first time a one to one representation of a star cluster.

We found that, on time-scales shorter than 1 Gyr, all the stars heavier than $30 M_{\odot}$ concentrate in the cluster centre on sub-pc scales, leading to the formation of a very dense, contracting core. Such a core alters the dynamics within the cluster, changing over relatively small times the cumulative mass distribution and the 3D velocity dispersion profile of the system.

The numerical results obtained support the statistical results presented above, suggesting that the observed correlation between star clusters and their centres is likely due to accumulation of heavy stars as consequence of mass segregation in a very small region ($\lesssim 0.1$ pc).

It is worth noting that the scaling relations reported here, in remarkably well agreement with observations, are similar to those connecting the mass of the central massive objects found in galactic nuclei and the mass of

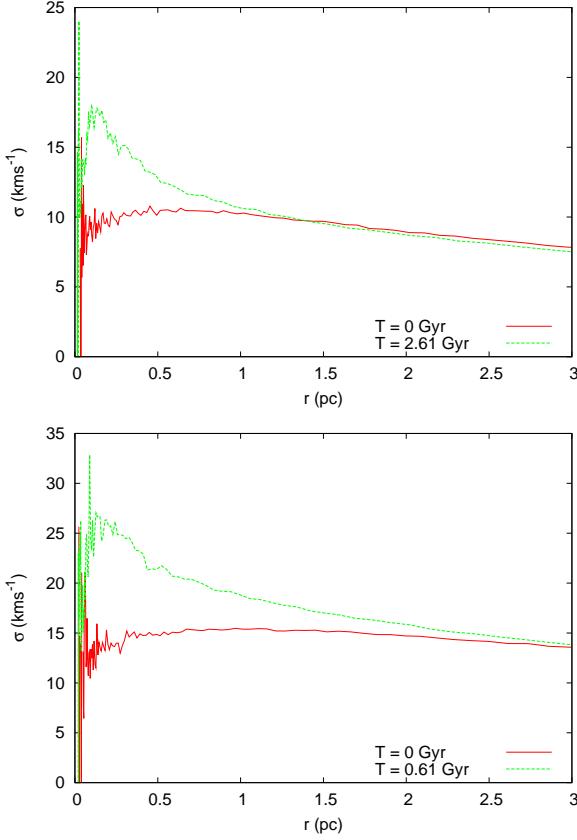


Figure 13. Velocity dispersion profile of the star cluster in case NB1 (top panel) and NB2 (bottom panel).

the galaxy in which they are observed (Côté et al. 2006; Ferrarese et al. 2006; Leigh et al. 2012; Scott & Graham 2013; Arca-Sedda & Capuzzo-Dolcetta 2014c). This similarity, argued also in other papers (see as example Barth et al. (2005); Safonova & Shastri (2010); Lützgendorf et al. (2013)), suggests that the presence of compact massive objects is a peculiarity of stellar systems on very different scales of mass, from stellar clusters to heavy galaxies.

In conclusions, this work showed for the first time that the concentration of massive stars within the centre of stellar clusters leads to the formation of compact systems composed by heavy stars, whose mass correlates with the mass of the host cluster as the observational evidences suggest.

ACKNOWLEDGEMENT

The author acknowledges R. Capuzzo-Dolcetta for his suggestions and comments which helped to improve the paper. The author acknowledges the MIUR which funded the research through the grant PRIN 2010 LY5N2T 005.

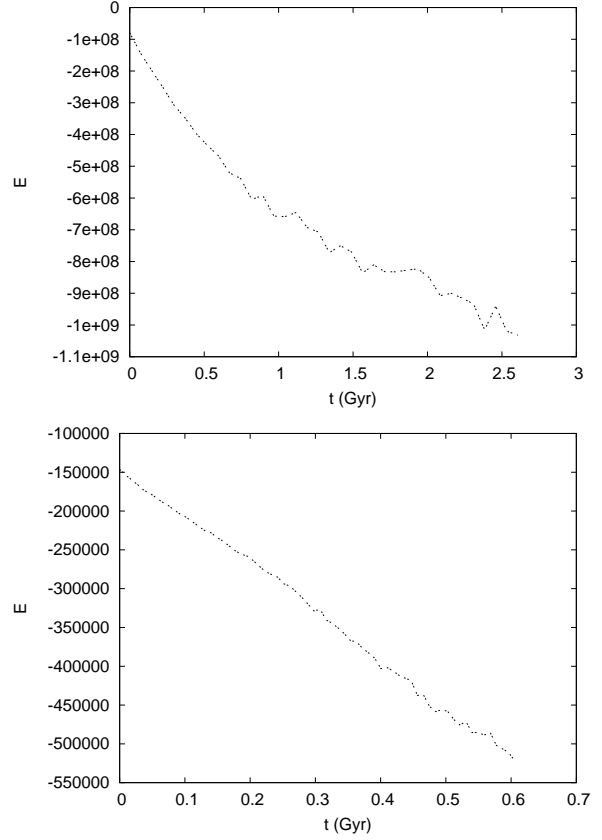


Figure 14. Total energy of the population of heavy stars in case NB1 (top panel) and NB2 (bottom panel).

Table 5.

Slope of the scaling relation between the mass of the cores and the cluster masses.

Model name	a	ϵ_a	b	ϵ_b
A1	1.0001	0.0015	-2.2283	0.0089
A2	0.9962	0.0016	-2.2498	0.0099
A3	0.9997	0.0014	-2.0454	0.0084
A4	0.99836	0.00097	-2.0746	0.0059
A5	1.006	0.013	-4.233	0.082
A6	0.985	0.043	-4.86	0.27
B1	1.0002	0.0012	-2.2017	0.0074
B2	0.9992	0.0014	-2.2383	0.0087
B3	0.99956	0.00080	-2.0242	0.0050
B4	1.0008	0.0011	-2.0663	0.0067
B5	0.997	0.014	-4.160	0.087
B6	0.972	0.032	-4.77	0.20

Column 1: model name. Column 2-3: slope of the fitting function and relative error. Column 4-5: offset of the fitting function and relative error.

Table 6.

The slope, a , of the relation $M_{IMBH} - M_{GC}$ evaluated by LU13

Method	a	ϵ_a
FITEXY	0.69	0.28
EM ALGORITHM	1.01	0.34
BUCLEY-JONES	0.96	0.32
BAYESIAN ANALYSIS	0.71	0.59

Column 1: name of the method used in LU13 to fit the correlation. Column 2-3: slope of the fitting relation and relative error.

REFERENCES

- Antonini F., 2013, *ApJ*, 763, 62
- Antonini F., Merritt D., 2012, *ApJ*, 745, 83
- Arca-Sedda M., Capuzzo-Dolcetta R., 2014a, *ApJ*, 785, 51
- Arca-Sedda M., Capuzzo-Dolcetta R., 2014b
- Arca-Sedda M., Capuzzo-Dolcetta R., 2014c, *MNRAS*, 444, 3738
- Barth A. J., Greene J. E., Ho L. C., 2005, *ApJL*, 619, L151
- Baumgardt H., Hut P., Makino J., McMillan S., Portegies Zwart S., 2003, *ApJL*, 582, L21
- Bekenstein J. D., 1973, *ApJ*, 183, 657
- Binney J., 1977, *MNRAS*, 181, 735
- Binney J., Tremaine S., 2008, *Galactic dynamics*. Princeton university press
- Brocato E., Castellani V., Raimondo G., Romaniello M., 1999, *A & A*, 136, 65
- Cappellari M., 2002, *MNRAS*, 333, 400
- Capuzzo-Dolcetta R., 1993, *ApJ*, 415, 616
- Capuzzo-Dolcetta R., Spera M., Punzo D., 2013, *Journal of Computational Physics*, 236, 580
- Chandrasekhar S., 1943a, *ApJ*, 97, 255
- Chandrasekhar S., 1943b, *ApJ*, 97, 263
- Chandrasekhar S., von Neumann J., 1943, *ApJ*, 97, 1
- Côté P., Piatek S., Ferrarese L., Jordán A., Merritt D., Peng E. W., Hasegan M., Blakeslee J. P., Mei S., West M. J., Milosavljević M., Tonry J. L., 2006, *ApJS*, 165, 57
- Dehnen W., 1993, *MNRAS*, 265, 250
- den Brok M., van de Ven G., van den Bosch R., Watkins L., 2014, *MNRAS*, 438, 487
- Emsellem E., Monnet G., Bacon R., 1994, *A & A*, 285, 723
- Feldmeier A., Lützgendorf N., Neumayer N., Kissler-Patig M., Gebhardt K., Baumgardt H., Noyola E., de Zeeuw P. T., Jalali B., 2013, *A & A*, 554, A63
- Ferrarese L., Côté P., Dalla Bontà E., Peng E. W., Merritt D., Jordán A., Blakeslee J. P., Hasegan M., Mei S., Piatek S., Tonry J. L., West M. J., 2006, *ApJL*, 644, L21
- Gebhardt K., Rich R. M., Ho L. C., 2002, *ApJL*, 578, L41
- Gebhardt K., Rich R. M., Ho L. C., 2005, *ApJ*, 634, 1093
- Gerssen J., van der Marel R. P., Gebhardt K., Guhathakurta P., Peterson R. C., Pryor C., 2002, *AJ*, 124, 3270
- Goswami S., Umbreit S., Bierbaum M., Rasio F. A., 2012, *ApJ*, 752, 43
- Gualandris A., Merritt D., 2008, *ApJ*, 678, 780
- Gürkan M. A., Freitag M., Rasio F. A., 2004, *ApJ*, 604, 632
- Hurley J. R., Pols O. R., Tout C. A., 2000, *MNRAS*, 315, 543
- Jeans J. H., 1916, *MNRAS*, 76, 552
- Kamann S., Wisotzki L., Roth M. M., Gerssen J., Husser T.-O., Sandin C., Weilbacher P., 2014, *A & A*, 566, A58
- Kroupa P., 2001, *MNRAS*, 322, 231
- Leigh N., Böker T., Knigge C., 2012, *MNRAS*, 424, 2130
- Leigh N. W. C., Lützgendorf N., Geller A. M., Maccarone T. J., Heinke C., Sesana A., 2014, *MNRAS*, 444, 29
- Lützgendorf N., Baumgardt H., Kruijssen J. M. D., 2013, *A & A*, 558, A117
- Lützgendorf N., Kissler-Patig M., Gebhardt K., Baumgardt H., Kruijssen D., Noyola E., Neumayer N., de Zeeuw T., Feldmeier A., van der Helm E., Pelupessy I., Portegies Zwart S., 2015, *ArXiv e-prints*
- Lützgendorf N., Kissler-Patig M., Gebhardt K., Baumgardt H., Noyola E., de Zeeuw P. T., Neumayer N., Jalali B., Feldmeier A., 2013, *A & A*, 552, A49
- Lützgendorf N., Kissler-Patig M., Neumayer N., Baumgardt H., Noyola E., de Zeeuw P. T., Gebhardt K., Jalali B., Feldmeier A., 2013, *AAP*, 555, A26
- Mapelli M., Bressan A., 2013, *MNRAS*, 430, 3120
- Mapelli M., Zampieri L., Ripamonti E., Bressan A., 2013, *MNRAS*, 429, 2298
- Merritt D., Graham A. W., Moore B., Diemand J., Terzić B., 2006, *AJ*, 132, 2685
- Miller M. C., Hamilton D. P., 2002, *MNRAS*, 330, 232
- Miller-Jones J. C. A., Wrobel J. M., Sivakoff G. R., Heinke C. O., Miller R. E., Plotkin R. M., Di Stefano R., Greene J. E., Ho L. C., Joseph T. D., Kong A. K. H., Maccarone T. J., 2012, *ApJL*, 755, L1
- Milosavljević M., Merritt D., 2001, *ApJ*, 563, 34
- Noyola E., Gebhardt K., Bergmann M., 2008, *ApJ*, 676, 1008
- Ostriker J. P., Binney J., Saha P., 1989, *MNRAS*, 241, 849
- Pesce E., Capuzzo-Dolcetta R., Vietri M., 1992, *MNRAS*, 254, 466
- Portegies Zwart S. F., Makino J., McMillan S. L. W., Hut P., 1999, *AAP*, 348, 117
- Safonova M., Shastri P., 2010, *Ap& SS*, 325, 47
- Salpeter E. E., 1955, *ApJ*, 121, 161
- Scott N., Graham A. W., 2013, *ApJ*, 763, 76
- Spitzer Jr. L., 1940, *MNRAS*, 100, 396
- Strader J., Chomiuk L., Maccarone T. J., Miller-Jones J. C. A., Seth A. C., 2012, *Nature*, 490, 71
- Tremaine S. D., 1976, *ApJ*, 203, 72
- Trenti M., van der Marel R., 2013, *MNRAS*, 435, 3272
- Vicari A., Capuzzo-Dolcetta R., Merritt D., 2007, *ApJ*, 662, 797
- Ziosi B. M., Mapelli M., Branchesi M., Tormen G., 2014, *MNRAS*, 441, 3703